Instanton Effects in QCD Sum Rules for the 0^{++} Hybrid

Zhu-feng Zhang[1], Qing Xu[2], Hong-ying Jin[2] and T. G. Steele[3]
[1]Physics Department, Ningbo University, Zhejiang Province, P. R. China
[2]Zhejiang Institute of Modern Physics, Zhejiang University, Zhejiang Province, P. R. China
[3] Department of Physics and Engineering Physics, University of Saskatchewan, Saskatoon, Saskatchewan, Canada S7N 5E2
(Dated: February 22, 2012)

In this paper, we study instanton contributions to the correlator of the hybrid current $g\bar{q}\sigma_{\mu\nu}G^a_{\nu\mu}T^a q$. These contributions are then included in a QCD sum-rule analysis of the isoscalar 0^{++} hybrid mass. We find a mass at 1.83 GeV for the $(\bar{u}ug+\bar{d}dg)/\sqrt{2}$ hybrid. However, for the $\bar{s}sg$ hybrid, we find the sum rules are unstable. We also study non-zero width effects, which affect the mass prediction. The mixing effects between these two states are studied and we find QCD sum rules support the existence of a flavor singlet hybrid with mass at around 1.9 GeV. Finally, we study the mixing effects between hybrid and glueball currents. The mixing between the $(\bar{u}ug+\bar{d}dg)/\sqrt{2}(\bar{s}sg)$ and the glueball causes two states, one in the region 1.4-1.8 GeV(1.4-2.2 GeV), and the other in the range 1.8-2.2 GeV(2.2-2.6 GeV).

PACS numbers: 12.38.Lg, 12.39.Mk

I. INTRODUCTION

It is generally believed that hadrons beyond the conventional quark model may exist. Theoretical predications of hybrid properties (mass, decay constant etc.) are therefore an important ingredient of their experimental confirmation.

Among these unconventional hadrons, the hybrids (first predicted in [1, 2]) have attracted considerable attention. Hybrid properties have been studied in many approaches, such as the Bag Model[3, 4], Potential Models[5] and QCD sum rules[6–8] (see [9–12] for the most recent works). Most studies have focused on hybrids with exotic quantum numbers (e.g., 1^{-+}) because such states do not mix with ordinary $\bar{q}q$ mesons. Less attention has been paid to the 0^{++} hybrid because it is experimentally very difficult to identify the composition of such a state, and it is also considered as a highly excited flux tube (e.g., some authors think the 0^{++} is one of the degenerate ground states in the flux tube model[13]).

Huang et al previously studied the hybrid with 0^{++} quantum numbers in the framework of QCD sum rules[14]. They used two currents: $g\bar{q}\sigma_{\mu\nu}G^a_{\nu\mu}T^a q$ and $g\bar{q}\gamma_\mu G^a_{\nu\mu}T^a q$. They found that the scalar current predicts $\bar{s}sg$ hybrid at a mass of $2.30-2.35$ GeV while the vector current predicts 3.4 GeV. The interesting thing is that the predicted 0^{++} hybrid mass ($2.30-2.35$GeV) is much lower than the previous predictions[15–19]. This 2.30 GeV prediction may be meaningful in experiments. From the particle data book, we find there are four 0^{++} mesons in the region 2000 MeV $\sim$ 2300 MeV. This is more crowded than the group of $f_0(1370)$, $f_0(1500)$ and $f_0(1710)$. Therefore, even if the glueball state is included, it is still hard to explain these four states. One possible explanation may be that there is a 0^{++} hybrid among them. But this picture is not compatible with the flux tube picture, so it is worth studying the 0^{++} hybrid mass in more detail.

The scalar channels are known to contain important effects from instantons[20, 21], which play an important role in the scalar glueball and pseudoscalar glueball calculations. Thus instantons may also be important for the 0^{++} hybrid. In this paper, we calculate such instanton effects to the correlator of the 0^{++} hybrid current $g\bar{q}\sigma_{\mu\nu}G^a_{\nu\mu}T^a q$. With our new result supplementing other known contributions, we calculate the hybrid mass with quark content u, d and s respectively. In addition, we study the effect of a Breit-Wigner form for the phenomenological spectral density. Flavor mixing effects between these two states are then studied in an attempt to give a prediction of the mass of flavor octet and singlet scalar hybrid. Finally, we study the mixing effects between hybrid and glueball currents.

II. THE MASSES OF THE PURE STATES: $(\bar{u}ug+\bar{d}dg)/\sqrt{2}$ AND $\bar{s}sg$

We start our QCD sum rule analysis by considering two scalar hybrid currents as used in Ref.[14] which are pure states in flavor space with isospin 0, i.e.,

$$j_1(x)=\frac{1}{\sqrt{2}}g[\bar{u}(x)\sigma_{\mu\nu}G^a_{\nu\mu}(x)T^a u(x)+\bar{d}(x)\sigma_{\mu\nu}G^a_{\nu\mu}(x)T^a d(x)], \tag{1}$$

and

$$j_2(x) = g\bar{s}(x)\sigma_{\mu\nu}G^a_{\nu\mu}(x)T^a s(x). \tag{2}$$

The first step of QCD sum rules is to use the operator-product expansion (OPE) to calculate the correlation function, which is defined as [22–24]:

$$\Pi(q^2) = \mathrm{i}\int \mathrm{d}^4x\, \mathrm{e}^{\mathrm{i}qx}\langle 0|Tj(x)j^\dagger(0)|0\rangle. \tag{3}$$

The imaginary part of the correlator (up to dimension 6 condensates) is given in [14]:

$$\mathrm{Im}\Pi(s)^{(\mathrm{OPE})} = \frac{\alpha_s(\mu^2)}{24\pi^2}s^3 + 4\alpha_s(\mu^2)m_q\langle\bar{q}q\rangle s - m_q^2\langle\alpha_s G^2\rangle + \frac{8\alpha_s(\mu^2)\pi^2}{3}m_q^2\langle\bar{q}q\rangle^2\delta(s), \tag{4}$$

where $q = u$ for j_1 and $q = s$ for j_2.

The second standard step of QCD sum rules is to combine the OPE-correlator with the phenomenological single narrow resonance spectral density ansatz

$$\mathrm{Im}\Pi(s)^{(\mathrm{phen})} = \pi f_H^2(m_H^2)^3\delta(s - m_H^2) + \mathrm{Im}\Pi(s)^{(\mathrm{OPE})}\theta(s - s_0) \tag{5}$$

via the Borel-transformed correlator

$$\hat{B}\Pi(q^2) \equiv \lim_{\substack{Q^2,n\to\infty \\ n/Q^2=\tau}} \frac{(Q^2)^{n+1}}{n!}\left(-\frac{\mathrm{d}}{\mathrm{d}Q^2}\right)^n \Pi(-Q^2) = \frac{1}{\pi}\int_0^\infty \mathrm{d}s\, \mathrm{e}^{-s\tau}\mathrm{Im}\Pi(s), \tag{6}$$

then we reach the sum rule:

$$f_H^2(m_H^2)^3\mathrm{e}^{-m_H^2\tau} + \frac{1}{\pi}\int_{s_0}^\infty \mathrm{d}s\, \mathrm{e}^{-s\tau}\mathrm{Im}\Pi(s)^{(\mathrm{OPE})} = \hat{B}\Pi(q^2)^{(\mathrm{OPE})}, \tag{7}$$

where s_0 is the threshold separating the contribution from higher excited states and the QCD continuum.

Notice that in Eq.(4), the leading-order mass corrections for the $\langle\alpha_s G^2\rangle$ term and $\langle\bar{q}q\rangle^2$ term, which should play an important role in the OPE of correlator, are not present (i.e., there is a chiral suppression of these terms). Because of the lack of these terms, the non-perturbative contributions may be underestimated. This defect may be improved by introducing instanton effects into the sum rules.

It has been known for a long time that the instanton plays an important role in the QCD vacuum and hadron physics[20, 21]. The explicit instanton in regular gauge can be expressed as

$$A^a_\mu(x;z) = \frac{2}{g}\frac{\eta_{a\mu\nu}(x-z)_\nu}{(x-z)^2 + \rho^2}, \tag{8}$$

where ρ is the instanton size, z is the position of the instanton center in Euclidean space, and η is the 't Hooft symbol.

If an instanton exists in space, quarks may occupy a special state called zero-mode state (one of each flavor). Usually, the quark zero-mode propagator is complicated, but if we deal with problems in the framework of Single-Instanton Approximation (SIA)[25], the propagator takes a simple form,

$$S(x,y;z) = \frac{\rho^2}{8\pi^2 m^\star}\frac{1}{((x-z)^2+\rho^2)^{3/2}((y-z)^2+\rho^2)^{3/2}}\left[\gamma^\mu\gamma^\nu\frac{1}{2}(1-\gamma^5)\right]\otimes(\tau^+_\mu\tau^-_\nu), \tag{9}$$

where $\tau^\pm = (\boldsymbol{\tau}, \mp\mathrm{i})$, and $m^\star$ is the quark effective mass which takes all the collective contribution of all instantons other than the leading one. For u, d quarks, after evaluating the effective mass in the Random Instanton Liquid Model and Interacting Instanton Liquid Model, Faccioli et al pointed out that $m^\star_u = 86\,\mathrm{MeV}$ should be used in the applications of SIA when two zero-mode propagators are involved [25]. However, in the present case, besides quark zero-modes, we also have direct instanton contributions from gauge field strength. This extra contribution may change the value of $m^\star$ away from 86 MeV. Thus, in this paper, we will still use the formerly widely used estimate by Shifman et al[26]:

$$m^\star_q = m_q - \frac{2}{3}\pi^2\rho^2\langle\bar{q}q\rangle. \tag{10}$$

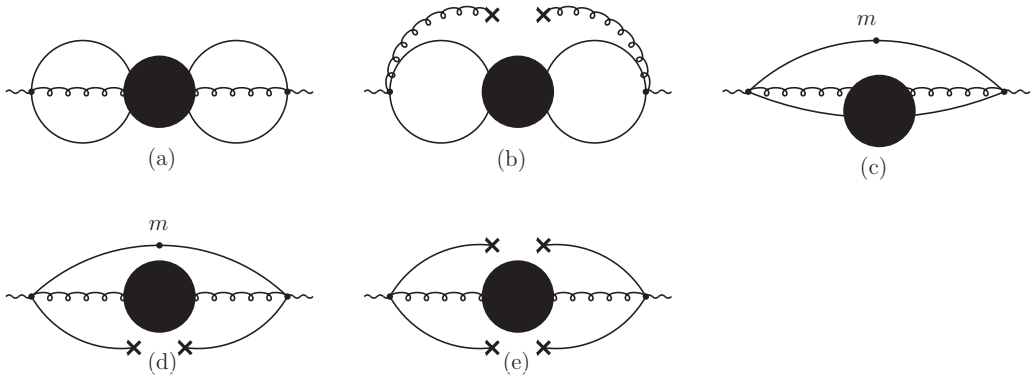

FIG. 1: Non-zero instanton contributions for the correlator of j_1 (Fig.(a-e)) or j_2 (Fig.(c-e)). (The blob denotes an instanton.)

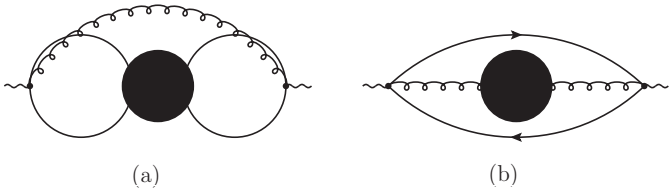

FIG. 2: Some zero instanton contributions.

Now let us consider the instanton contributions to the correlation functions of currents j_1 and j_2. In Fig.1 we draw some diagrams which are associated with nonvanishing contributions. The instanton contributions originating from Fig.1(a-b) only play a role in the correlator of j_1, while Fig.1(c-e) contribute to both j_1 and j_2. There are many other figures with vanishing contributions to the correlator (e.g. Fig.2) that explains why the leading-order mass corrections to the $\langle\bar{q}q\rangle^2$ and $\langle\alpha_s G^2\rangle$ condensates in Eq. (4) do not appear.

Among these instanton contributions, the most important one for j_1 comes from Fig.1(a), which reads

$$\Pi(q^2)^1_{j_1} = \frac{1}{2}\int \mathrm{d}\rho \frac{n(\rho)\rho^2}{m_u^{\star 2}} Q^6 K_3^2(Q\rho), \tag{11}$$

where $n(\rho)$ is the density of instantons. We get the imaginary part of $\Pi(q^2)^1_{j_1}$ upon analytic continuation to the physical domain,

$$\mathrm{Im}\Pi(s)^1_{j_1} = -\int \mathrm{d}\rho \frac{n(\rho)\rho^2\pi^2}{4m_u^{\star 2}} s^3 J_3(\sqrt{s}\rho) Y_3(\sqrt{s}\rho). \tag{12}$$

Usually one uses the simple spike distribution $n(\rho) = \bar{n}\delta(\rho - \bar{\rho})$, where $\bar{n} = 8\times 10^{-4}\,\mathrm{GeV}^4$ is the average instanton density and $\bar{\rho} = 1/(0.6\,\mathrm{GeV})$ is the average instanton size. Notice that the instanton contributions (Eq.(12) and that from the other three diagrams) are oscillating functions, of which the amplitude becomes larger along with s in some regions where the spectral density is negative. This problem also arises in other cases, for instance see [27, 28]. This situation is called local duality violation [29]. One approach used to mitigate this unphysical tendency introduces a distribution function of the instanton, for instance, in Ref.[27], the author used a gaussian-tail distribution

$$n(\rho) = \frac{2^{18}}{3^6\pi^3}\frac{\bar{n}}{\bar{\rho}}\left(\frac{\rho}{\bar{\rho}}\right)^4 \mathrm{e}^{-2^6\rho^2/(3^2\pi\bar{\rho}^2)} \tag{13}$$

in the analysis of QCD sum rules for glueball, which improves the physical tendency of the spectral density. However, this approach of a modified instanton distribution does not seem to be intrinsically necessary. For example, local dulaity violation has also been addressed by constructing differently-weighted sum-rules [28]. For the cases we are studying, the gaussian tail distribution does not work.

In our case, the amplitude of the instanton-induced spectral density does not decline quickly when s becomes larger; this means the contributions from large instantons are not suppressed, and thus the single instanton approximation is not appropriate in the Minkowski domain. However, in the deep Euclidean domain, instanton contributions are

exponentially suppressed, and the single instanton approximation works well. That means global duality is not violated although local duality is strongly violated in the single instanton approximation. Because QCD sum rules are based global duality, the single instanton approximation should be appropriate.

Based on the considerations above, we deal with instanton contributions in the Euclidean domain in this paper, i.e., we introduce $\hat{B}\Pi(q^2)^{(\rm inst)}$ to the right hand side of Eq.(7) directly as in Ref.[30–32], and we still use spike distribution. All Borel-transformed instanton contributions are listed as follows

$$\hat{B}\Pi(q^2)^{\rm Fig.1(a)} = \frac{4\bar{n}}{m_q^{\star 2}\bar{\rho}^6}{\rm e}^{-\xi}\xi^5\left[\xi(1+4\xi)K_0(\xi)+(2+3\xi+4\xi^2)K_1(\xi)\right], \tag{14}$$

$$\hat{B}\Pi(q^2)^{\rm Fig.1(b)} = \frac{\bar{n}\pi}{m_q^{\star 2}\bar{\rho}^2}\langle\alpha_s G^2\rangle\,{\rm e}^{-\xi}\xi^3\left[K_0(\xi)+K_1(\xi)\right], \tag{15}$$

$$\hat{B}\Pi(q^2)^{\rm Fig.1(c)} = \frac{2048}{25\pi}\frac{\bar{n}}{\bar{\rho}^4}\frac{m_q}{m_q^\star}{\rm e}^{-\xi}\xi^3(1+4\xi)K_{1/2}(\xi), \tag{16}$$

$$\hat{B}\Pi(q^2)^{\rm Fig.1(d)} = -64\bar{n}\pi^2\langle m_q\bar{q}q\rangle\,{\rm e}^{-\xi}\xi K_0(\xi), \tag{17}$$

$$\hat{B}\Pi(q^2)^{\rm Fig.1(e)} = -\frac{128}{3}\bar{n}\pi^4\bar{\rho}^2\langle\bar{q}q\rangle^2\,{\rm e}^{-\xi}\xi K_0(\xi), \tag{18}$$

where $\xi=\bar{\rho}^2/(2\tau)$.

Finally, we should include instanton contributions in our sum rules very carefully to avoid double counting. If we accept the assumption that operator condensates are induced by instantons, then the contributions from Fig.1(a) and (b) (Fig.1(c) and (d)) have double counting, and we should only consider the former contribution. Fig.1(e) is a special case. In the OPE, the four quark condensate can be composed of the same four quarks. Such a four quark condensate cannot be induced in the single instanton picture because one quark can occupy only one zero-mode state in an instanton, thus it seems that we should still retain this Fig.1(e) contribution. However, the quark effective mass takes the collective contribution of all instantons other than the leading one in SIA, thus we cannot exclude the possibility of double counting between Fig.1(a) and (e), an issue that deserves further study beyond the scope of this paper. Luckily, in the present case, including/excluding the contribution from Fig.1(e) does not significantly influence sum rules in most cases (e.g. $(\bar{u}ug+\bar{d}dg)/\sqrt{2}$), thus we will include Fig.1(e) in our calculation.

Based on the above considerations, we take the following final instanton contributions for current j_1:

$$\hat{B}\Pi(q^2)^{(\rm inst)}_{j_1} = \hat{B}\Pi(q^2)^{\rm Fig.1(a)} + \hat{B}\Pi(q^2)^{\rm Fig.1(c)} + \hat{B}\Pi(q^2)^{\rm Fig.1(e)}, \tag{19}$$

where all $q=u$, while for j_2

$$\hat{B}\Pi(q^2)^{(\rm inst)}_{j_2} = \hat{B}\Pi(q^2)^{\rm Fig.1(c)} + \hat{B}\Pi(q^2)^{\rm Fig.1(e)}, \tag{20}$$

where all $q=s$.

Now the mass of the hybrid m_H can be expressed in the form of

$$m_H = \sqrt{\frac{R_1(\tau,s_0)^{(\rm OPE)} + (-\partial/\partial\tau)\hat{B}\Pi(q^2)^{(\rm inst)}}{R_0(\tau,s_0)^{(\rm OPE)} + \hat{B}\Pi(q^2)^{(\rm inst)}}}, \tag{21}$$

where the moments $R_k^{(\rm OPE)}$ is defined as

$$R_k(\tau,s_0)^{(\rm OPE)} = \frac{1}{\pi}\int_0^{s_0}{\rm d}s\,s^k{\rm e}^{-s\tau}{\rm Im}\Pi(s)^{(\rm OPE)},\ k=0,1. \tag{22}$$

The single narrow resonance spectral density (5) is an over-simplified model, so sometimes a Breit-Wigner (BW) form spectral density is used in QCD sum rules[33–38]. In this paper, we also study whether the hybrid mass prediction is sensitive to this form of the spectral density. The only thing we need to do is replace $\delta(s-m_H^2)$ in the spectral density with

$$\frac{1}{\pi}\frac{m_H\Gamma}{(s-m_H^2)^2+m_H^2\Gamma^2}, \tag{23}$$

where Γ is the width of the hybrid[39]. Notice that if $\Gamma\to 0$, we can get a delta-type function again.

In this BW-type spectral density model, we should compare

$$\frac{\int_0^{s_0} s\,{\rm e}^{-s\tau}/[(s-m_H^2)^2+m_H^2\Gamma^2]{\rm d}s}{\int_0^{s_0}{\rm e}^{-s\tau}/[(s-m_H^2)^2+m_H^2\Gamma^2]{\rm d}s} \tag{24}$$

with the square of the right hand side of Eq.(21) to get the QCD sum rules. In the QCD sum rules window, the two quantities should be equal.

Before presenting the numerical results, we should fix the values of various phenomenological parameters which appear in our sum rules. The condensates and constants are chosen as follows[22, 23]

$$\begin{aligned}&\Lambda_{\rm QCD} = 0.2\,{\rm GeV}, \quad m_u = 5\,{\rm MeV}, \quad m_s = 150\ {\rm MeV},\\ &\langle\bar{u}u\rangle = -(0.25\,{\rm GeV})^3, \quad \langle\bar{s}s\rangle = 0.8\langle\bar{u}u\rangle, \quad \langle\alpha_s G^2\rangle/\pi = 0.012\,{\rm GeV}^4.\end{aligned} \tag{25}$$

Renormalization-group (RG) improvement of the sum rules amounts to substitutions $\mu^2 \to 1/\tau$ in Eq.(4), i.e.,

$$\alpha_s(\mu^2) \to \alpha_s(1/\tau) = -\frac{4\pi}{9\ln(\tau\Lambda^2_{\rm QCD})}. \tag{26}$$

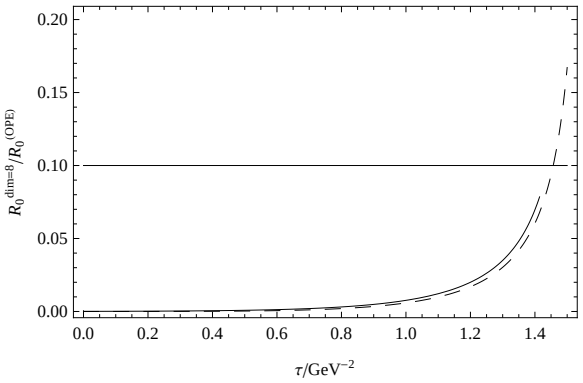

FIG. 3: The solid line, the dashed line denote $R_0^{\rm dim=8\ operator}/R_0^{\rm (OPE)}$ for j_2 with $s_0 = 6.0\,{\rm GeV}^2$ and $s_0 = 12.0\,{\rm GeV}^2$ respectively.

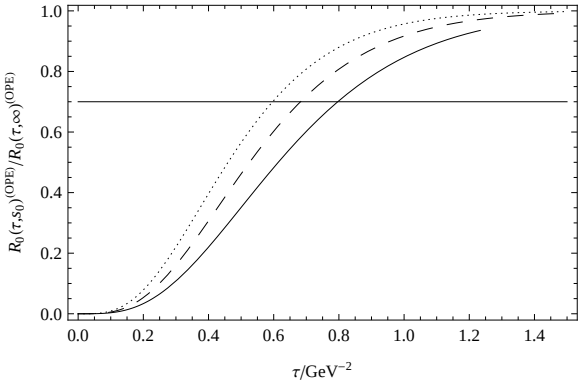

FIG. 4: The solid line, the dashed line and the dotted line denote $R_0(\tau, s_0)^{\rm (OPE)}/R_0(\tau,\infty)^{\rm (OPE)}$ for j_1 with $s_0 = 6.0\,{\rm GeV}^2$, $7.0\,{\rm GeV}^2$ and $8.0\,{\rm GeV}^2$ respectively.

Finally, we should determine the QCD sum rules window. To establish our sum rules, the Borel parameter τ should not be too large, else the convergence of $R_k(\tau, s_0)^{\rm (OPE)}$ will be destroyed because of effects from the omitted higher dimension condensates in our calculation. Luckily, in the present cases, the convergence of the OPE series is very good because of the small value of light quark masses. We make an estimate by demanding that the contribution from the dimension 8 operator, i.e., $\langle m_q\bar{q}q\rangle^2$, for the sum-rule moment R_0 should be less than 10% of the total OPE contribution. From Fig.3, we find $\tau = 1.4\,{\rm GeV}^{-2}$ is an appropriate upper bound for j_2 (for current j_1, we can choose a larger value for the upper bound.). Meanwhile, τ should not be too small, else the continuum contribution will be too large. We demand the continuum contribution is less than 30% of the total contributions[40, 41]. From Fig.4 we find $\tau = 0.8\,{\rm GeV}^{-2}$ is an appropriate lower bound for j_1 with $s_0 = 6.0\,{\rm GeV}^2$. If we choose a larger s_0, the lower bound of τ can be reduced to a smaller value. For the current j_2, the lower bound of τ is almost the same. Finally, we also should remember the continuum threshold s_0 should be larger than m_H^2.

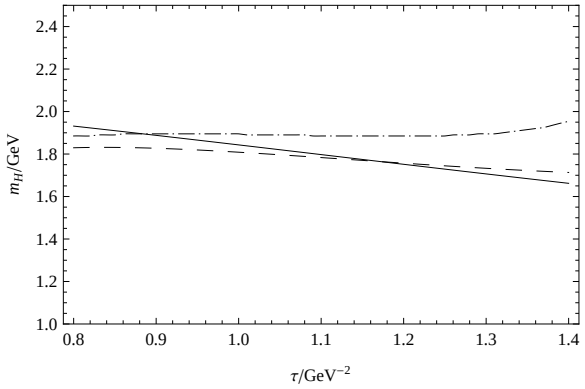

FIG. 5: The sum rules for j_1. The solid line, the dashed line and the dot-dashed line denote the sum rule without instanton contributions, with instanton contributions and the BW-type sum rule (with instanton contributions) respectively. We choose $s_0 = 6.0\,\mathrm{GeV}^2$ and $\Gamma = 0.04\,\mathrm{GeV}$.

In Fig.5 we show the sum rules for j_1. From this figure we find that without instanton contributions, the sum rule is very unstable. After including instanton contributions, we find an improved sum rule which gives a mass at about $1.83\,\mathrm{GeV}$ for the scalar hybrid $(\bar{u}ug + \bar{d}dg)/\sqrt{2}$. We should emphasize that, after including instanton contributions, the sum rule is less sensitive to variation in s_0 than the sum rule without these effects (see Fig.6). We also show the BW-type sum rule in Fig.5. The dot-dashed lines shows the fitted mass for the hybrid in demanding that the difference between Eq.(24) and the square of the right hand side of Eq.(21) is less than $0.01\,\mathrm{GeV}^2$. We find a heavier mass for the hybrid, about $1.88\,\mathrm{GeV}$. This tendency of width effects to increase the sum-rule mass determination has also been observed for 0^{++} $\bar{q}q$ mesons [42]. We also find for larger or smaller Γ, the sum rules lose their stability in the sum rules window.

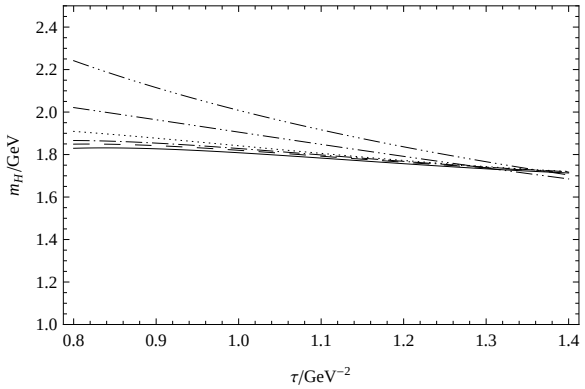

FIG. 6: The sum rules with instanton contributions for j_1 with $s_0 = \{6.0,\ 7.0,\ 8.0,\ \infty\}\,\mathrm{GeV}^2$ for the {solid line, dashed line, dot-dashed line, dotted line} respectively, and the sum rules without instanton contributions for j_1 with $s_0 = \{7.0,\ \infty\}\,\mathrm{GeV}^2$ for the {dot-dot-dashed, dot-dot-dot-dashed line} respectively.

From Fig.7 we find after including the instanton contributions, the stability of the mass sum rule of j_2 becomes questionable. This fact may suggest that there are still other effects which are missing in our sum rules, a point which needs further study. However, if we choose $\Gamma = 0.08\,\mathrm{GeV}$, we find the result for the BW-type sum rule in the region $0.6\,\mathrm{GeV}^2 < \tau < 1\,\mathrm{GeV}^2$ is almost the same as the mass sum rule without instanton effects in Ref.[14], which gives a mass at about 2.20-2.30 GeV.

If we omit the contribution from Fig.1(e), the sum rule becomes more unstable, but the BW-type sum rule in the region $0.6\,\mathrm{GeV}^2 < \tau < 0.9\,\mathrm{GeV}^2$ gives a mass of about 2.30-2.35 GeV.

III. THE FLAVOR OCTET AND SINGLET OF THE SCALAR HYBRID

In the previous section, studying the sum rules for current j_1 and j_2 revealed that sum rules support the existence of the state associated with j_1 while the one associated with j_2 needs further confirmation.

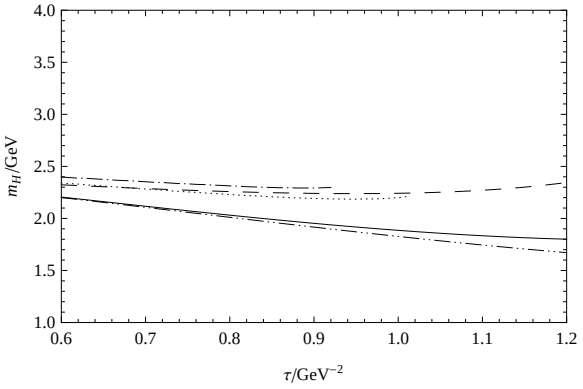

FIG. 7: The sum rules for j_2. The solid line, the dashed line denote sum rule with and without instanton contributions ($s_0 = 8.0\,\mathrm{GeV}^2$) respectively. The dotted line denotes the BW-type sum rule ($s_0 = 8.0\,\mathrm{GeV}^2$, $\Gamma = 0.08\,\mathrm{GeV}$). The dot-dot-dashed line and the dot-dashed line denote sum rule ($s_0 = 8.0\,\mathrm{GeV}^2$) and BW-type sum rule ($s_0 = 8.0\,\mathrm{GeV}^2, \Gamma = 0.11\,\mathrm{GeV}^2$) with instanton contributions (without contribution from Fig.1(e)) respectively.

The current j_1 and j_2 have the same quantum numbers, so they will mix with each other. In this section, we consider this mixing effect to predict the mass of hybrid in flavor octet and flavor singlet configurations. For this purpose, we consider the isospin 0 scalar hybrid current in the general form

$$j(x) = \frac{g}{\sqrt{2c_1^2 + c_2^2}} \left\{ c_1 \left[\bar{u}(x)\sigma_{\mu\nu} G^a_{\nu\mu}(x) T^a u(x) + \bar{d}(x)\sigma_{\mu\nu} G^a_{\nu\mu}(x) T^a d(x) \right] + c_2 \bar{s}(x)\sigma_{\mu\nu} G^a_{\nu\mu}(x) T^a s(x) \right\}, \tag{27}$$

where c_1 and c_2 are two adjustable parameters. For $c_1 = 1$ and $c_2 = 0$ ($c_1 = 0$ and $c_2 = 1$), we get our current j_1 (j_2) studied in the previous section. For $c_1 = 1$ and $c_2 = -2$ we get the flavor octet hybrid, and for $c_1 = c_2 = 1$, the hybrid becomes a flavor singlet one.

The mixing effect between j_1 and j_2 can be described by the correlator

$$\Pi(q^2)^{(\mathrm{mix})} = \mathrm{i} \int \mathrm{d}^4x\, \mathrm{e}^{\mathrm{i}qx} \langle 0 | T j_1(x) j_2^\dagger(0) | 0 \rangle, \tag{28}$$

which will not receive any contribution from perturbative theory. But it does receive instanton contributions, which is similar to contributions from Fig.1(a), with one s-quark loop and one u-quark (or d-quark) loop in zero-mode states. The contribution can be read from Eq.(14)

$$\hat{B}\Pi(q^2)^{(\mathrm{inst})}_{\mathrm{mix}} = \hat{B}\Pi(q^2)^{\mathrm{Fig.1(a)}} \tag{29}$$

with a replacement rule: $m_q^{\star 2} \to m_u^\star m_s^\star$.

Combining all contributions together, we get the final result for current j:

$$\begin{aligned} \mathrm{Im}\Pi(s)^{(\mathrm{OPE})} = {} & \frac{2c_1^2}{2c_1^2 + c_2^2} \left[\frac{\alpha_s}{24\pi^2} s^3 + 4\alpha_s m_u \langle \bar{u}u \rangle s - m_u^2 \langle \alpha_s G^2 \rangle + \frac{8\alpha_s \pi^2}{3} m_u^2 \langle \bar{u}u \rangle^2 \delta(s) \right] \\ & + \frac{c_2^2}{2c_1^2 + c_2^2} \left[\frac{\alpha_s}{24\pi^2} s^3 + 4\alpha_s m_s \langle \bar{s}s \rangle s - m_s^2 \langle \alpha_s G^2 \rangle + \frac{8\alpha_s \pi^2}{3} m_s^2 \langle \bar{s}s \rangle^2 \delta(s) \right], \end{aligned} \tag{30}$$

and

$$\hat{B}\Pi(q^2)^{(\mathrm{inst})}_j = \frac{2c_1^2}{2c_1^2 + c_2^2} \hat{B}\Pi(q^2)^{(\mathrm{inst})}_{j_1} + \frac{c_2^2}{2c_1^2 + c_2^2} \hat{B}\Pi(q^2)^{(\mathrm{inst})}_{j_2} + \frac{4c_1 c_2}{2c_1^2 + c_2^2} \hat{B}\Pi(q^2)^{(\mathrm{inst})}_{\mathrm{mix}}. \tag{31}$$

We plot the sum rules for the flavor octet isoscalar hybrid in Fig.8 and the flavor singlet state in Fig.9. From Fig.8 we find the mass upper bound ($s_0 \to \infty$) of the flavor octet hybrid is smaller than that with a finite s_0. Since this behaviour is unphysical, we conclude that this state is not supported by QCD sum rules.

From Fig.9 we find the mass of the flavor singlet hybrid is not very sensitive to s_0 in our sum rules window. Choosing $s_0 = 11.0\,\mathrm{GeV}^2$ as a typical s_0 value, from Fig.10 we get a flavor singlet hybrid mass at 1.86 GeV. If we use a BW-type sum rule with $\Gamma = 0.04\,\mathrm{GeV}$, we get a heavier mass, about 1.92 GeV.

Omitting the contribution from Fig.1(e) does not change the sum rule a lot, but it does allow a large width ($\Gamma = 0.06\,\mathrm{GeV}$), which leads to a mass at about 1.95 GeV.

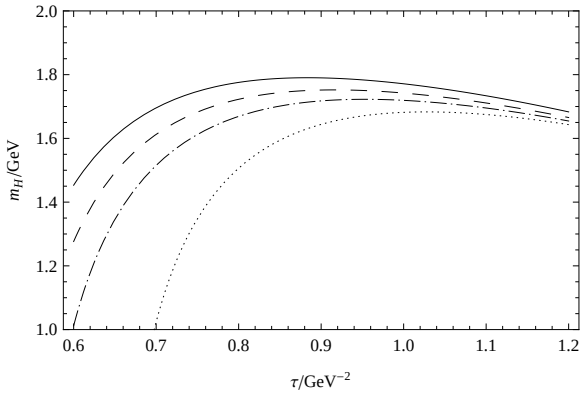

FIG. 8: The sum rules for the flavor octet hybrid with $s_0 = \{6.0,\ 7.0,\ 8.0,\ \infty\}\,\mathrm{GeV}^2$ for the {solid line, dashed line, dot-dashed line, dotted line} respectively.

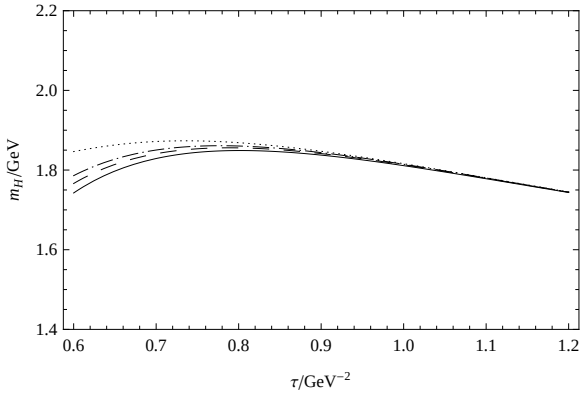

FIG. 9: The sum rules for the flavor singlet hybrid with $s_0 = \{9.0,\ 10.0,\ 11.0,\ \infty\}\,\mathrm{GeV}^2$ for the {solid line, dashed line, dot-dashed line, dotted line} respectively.

IV. MIXING WITH SCALAR GLUEBALL

The hybrid currents j_1 and j_2 may also mix with the glueball current (32). From the perspective of perturbation theory, such a mixing is chirally suppressed, so the mixing must be non-perturbative if it is not small. In our framework, the mixing between the scalar hybrid and the scalar glueball may occur through instanton and quark condensate effects. In this section, we discuss how instanton and quark condensate contributions affect the sum rules. With this motivation, we consider a scalar current[43]

$$j_{0^{++}} = \beta j_{\rm hybrid} + (1-|\beta|) M_0 j_{\rm glueball}, \tag{32}$$

where $j_{\rm glueball} = \alpha_s G^2$ is the scalar glueball current, M_0 is a parameter which has the dimension of the mass while β is a parameter which can run from -1 to 1.

All contributions for the glueball correlator already exist in literature, e.g., the OPE contribution to the glueball current correlator reads (up to dimension 8 condensate) [44, 45]:

$$\begin{aligned} R_0(\tau,s_0)^{\rm (OPE)}_{\rm glueball} = \int_0^{s_0} {\rm d}s\, s^2 {\rm e}^{-s\tau} \left\{ 2\left(\frac{\alpha_s}{\pi}\right)^2 \left[1+\frac{659}{36}\frac{\alpha_s}{\pi}+247.48\left(\frac{\alpha_s}{\pi}\right)^2\right] - 4\left(\frac{\alpha_s}{\pi}\right)^3 \left(\frac{9}{4}+65.781\frac{\alpha_s}{\pi}\right)\ln\frac{s}{\mu^2} \right. \\ \left. - 10.125\left(\frac{\alpha_s}{\pi}\right)^4 \left(\pi^2 - 3\ln^2\frac{s}{\mu^2}\right)\right\} + 9\pi\left(\frac{\alpha_s}{\pi}\right)^2 \langle\alpha_s G^2\rangle \int_0^{s_0} {\rm d}s\, {\rm e}^{-s\tau} + 8\pi^2\left(\frac{\alpha_s}{\pi}\right)^2 \langle\mathcal{O}_6\rangle + 8\pi^2\frac{\alpha_s}{\pi}\langle\mathcal{O}_8\rangle\tau, \end{aligned} \tag{33}$$

where $\langle\mathcal{O}_6\rangle = \langle g_s f_{abc} G^a_{\mu\nu} G^b_{\nu\rho} G^c_{\rho\mu}\rangle = (0.27\,\mathrm{GeV}^2)\langle\alpha_s G^2\rangle$ and $\langle\mathcal{O}_8\rangle = 14\langle(\alpha_s f_{abc} G^a_{\mu\nu} G^b_{\nu\rho})^2\rangle - \langle(\alpha_s f_{abc} G^a_{\mu\nu} G^b_{\rho\lambda})^2\rangle =$

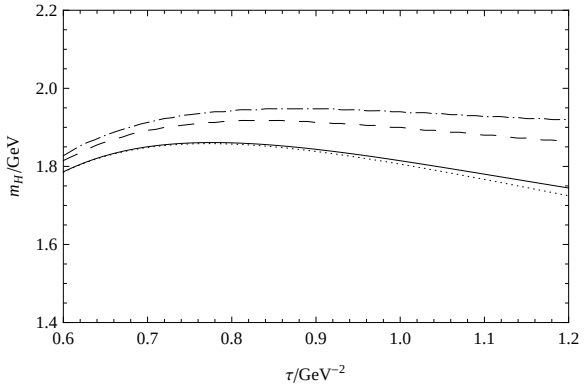

FIG. 10: The sum rules for the flavor singlet hybrid. The solid line, dashed line denote sum rule ($s_0 = 11.0\,\mathrm{GeV}^2$), BW-type sum rule ($s_0 = 11.0\,\mathrm{GeV}^2$ and $\Gamma = 0.04\,\mathrm{GeV}$) respectively. The dotted line and dot-dashed line denote sum rule ($s_0 = 11.0\,\mathrm{GeV}^2$), BW-type sum rule ($s_0 = 11.0\,\mathrm{GeV}^2$ and $\Gamma = 0.06\,\mathrm{GeV}$) without contribution from Fig.1(e) respectively.

$\frac{9}{16}(\langle\alpha_s G^2\rangle)^2$, and the instanton contribution to the glueball current correlator is[46]:

$$\hat{B}\Pi(q^2)_{\mathrm{glueball}} = \frac{256\bar{n}\pi^2}{\bar{\rho}^2}\mathrm{e}^{-\xi}\xi^5\left[K_0(\xi) + \left(1+\frac{1}{2\xi}\right)K_1(\xi)\right]. \tag{34}$$

The only unknown new term is the mixing contribution between hybrid and glueball

$$\Pi(q^2)_{\text{H-GB}} = \mathrm{i}\int \mathrm{d}^4x\,\mathrm{e}^{\mathrm{i}qx}\langle 0|Tg\bar{q}(x)\sigma_{\mu\nu}G^a_{\nu\mu}(x)T^a q(x)\alpha_s G(0)^2|0\rangle, \tag{35}$$

after some calculations, we get its contribution:

$$\hat{B}\Pi^{(\mathrm{inst})}_{\text{H-GB}} + R_0(\tau,s_0)^{(\mathrm{OPE})}_{\text{H-GB}} = -\frac{16\bar{n}\pi}{m_q^\star\bar{\rho}^4}\{\xi^3 - \xi^4\mathrm{e}^{-\xi}[\xi(1+4\xi)K_0(\xi) + (2+3\xi+4\xi^2)K_1(\xi)]\} - 8\pi\left(\frac{\alpha_s}{\pi}\right)^2\frac{\langle\bar{q}q\rangle}{\tau^2}[1-\mathrm{e}^{-s_0\tau}(1+s_0\tau)]. \tag{36}$$

Although the mixed condensate can also avoid chiral suppression, its leading order contribution is zero after Borel transforming.

Before proceeding with the numerical calculations, let us fix the parameter M_0. Actually, the value of M_0 does not affect the sum rules because there is another parameter β. For convenience (so that β can approximately represent the mixing intensity), we choose $M_0 = 0.02\,\mathrm{GeV}$ so that the leading contributions of hybrid correlator and glueball correlator ($\alpha_s s^3/(24\pi^2)$ and $M_0 \cdot 2\alpha_s^2 s^2/\pi$) are the same order of magnitude at this scale, where we choose $\mu = 1\,\mathrm{GeV}$ in this section, and α_s is fixed to 0.517.

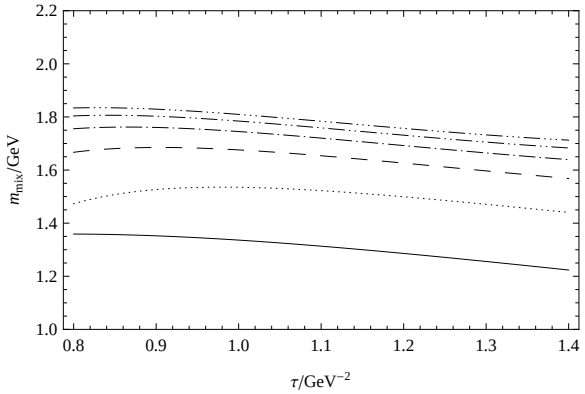

FIG. 11: The sum rules for the mixing state of $\frac{1}{\sqrt{2}}(\bar{u}ug + \bar{d}dg)$ and the scalar glueball ($j = \beta j_1 + (1-|\beta|)j_{\mathrm{glueball}}$, $s_0 = 6.0\,\mathrm{GeV}^2$) with $\beta = \{0,\ 0.2,\ 0.4,\ 0.6,\ 0.8,\ 1\}$ for the {solid line, dotted line, dashed line, dot-dashed line, dot-dot-dashed line, dot-dot-dot-dashed line} respectively.

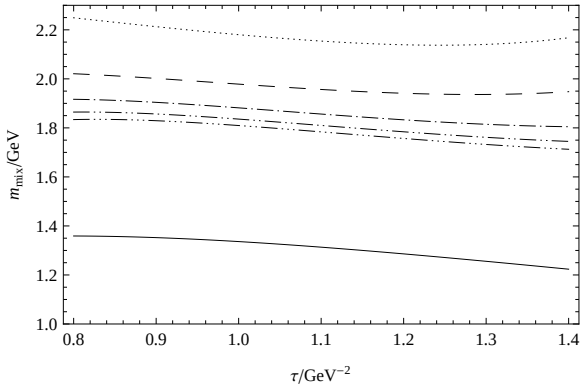

FIG. 12: The sum rules for the mixing state of $\frac{1}{\sqrt{2}}(\bar{u}ug+\bar{d}dg)$ and the scalar glueball ($j=\beta j_1+(1-|\beta|)j_{\rm glueball}$, $s_0=6.0\,{\rm GeV}^2$) with $\beta=\{0,\ -0.2,\ -0.4,\ -0.6,\ -0.8,\ -1\}$ for the {solid line, dotted line, dashed line, dot-dashed line, dot-dot-dashed line, dot-dot-dot-dashed line} respectively.

In Fig.11 and Fig.12 we show our result for the mixed state of $\frac{1}{\sqrt{2}}(\bar{u}ug+\bar{d}dg)$ and glueball. From Fig.11 we find that if $0<\beta<1$, then the mass of the mixed state will lie in the region 1.35-1.83 GeV, which covers the masses of $f_0(1370)$, $f_0(1500)$ and $f_0(1710)$. For example, the mass of the mixed state with $\beta=0.4$ is very close to the mass of $f_0(1710)$. From Fig.12 we find if $0>\beta>-1$, then the mass of the mixed state will lie in the region 1.83-2.2 GeV. Actually we find for $\beta>-0.2$, the sum rules are unstable. This fact is quite understandable. In the region $0>\beta>-1$, when β goes to zero, the content of the glueball increases and the expected mass goes up. Meanwhile according to the result in the region $0<\beta<1$, the expected mass must go down when β is very close to zero,. This contradictory causes the sum rules unstable. In other words, the content of the hybrid must dominate in the region $0>\beta>-1$. Clearly, after the mixing is taken into account, there are two states. One, dominated by the glueball content, is lighter, and may be $f_0(1370)$, $f_0(1500)$ and $f_0(1710)$; another one, dominated by hybrid content, is in region 1.83-2.2 GeV. It seems straightforward to extend our discussion to the mixing between the scalar hybrid and the normal $\bar{q}q$ scalar, however, there is a problem for such an extension because in our framework it is hard to identify the $\bar{q}q$ scalar in the group of $f_0(1370)$, $f_0(1500)$ and $f_0(1710)$ and in the region 2000 MeV $\sim$ 2300 MeV (both of which may mix with the hybrid). Certainly, this argument is also valid for the mixing between the glueball and the hybrid if there are two glueballs in these two groups respectively.

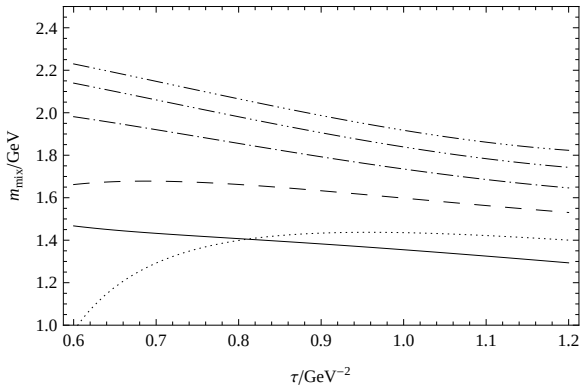

FIG. 13: The sum rules for the mixing state of $\bar{s}sg$ and the scalar glueball ($j=\beta j_2+(1-|\beta|)j_{\rm glueball}$, $s_0=8.0\,{\rm GeV}^2$) with $\beta=\{0,\ 0.2,\ 0.4,\ 0.6,\ 0.8,\ 1\}$ for the {solid line, dotted line, dashed line, dot-dashed line, dot-dot-dashed line, dot-dot-dot-dashed line} respectively.

Similarly, from Fig.13 and Fig.14 we learn that the mass of the mixed state of $\bar{s}sg$ and glueball is in the range 1.4-2.6 GeV, which may also shed light on the explanation of the contents of these light f_0 mesons.

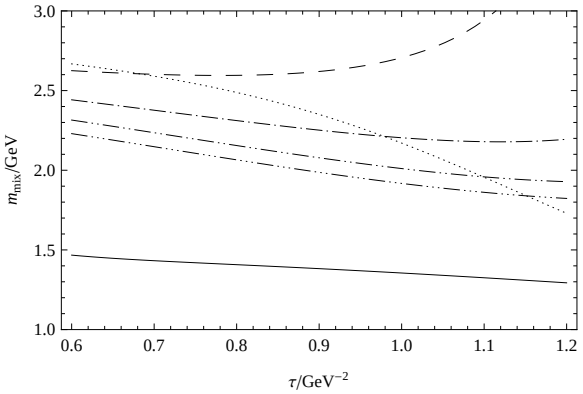

FIG. 14: The sum rules for the mixing state of $\bar{s}sg$ and the scalar glueball ($j = \beta j_2 + (1-|\beta|)j_{\rm glueball}$, $s_0 = 8.0\,{\rm GeV}^2$) with $\beta = \{0, \ -0.2, \ -0.4, \ -0.6, \ -0.8, \ -1\}$ for the {solid line, dotted line, dashed line, dot-dashed line, dot-dot-dashed line, dot-dot-dot-dashed line} respectively.

V. DISCUSSION AND SUMMARY

In this paper, we have calculated instanton contributions to the sum rules for the scalar hybrid. We find that instanton effects play an important role in the sum rule mass predictions for $(\bar{u}ug + \bar{d}dg)/\sqrt{2}$ hybrids. The sum rules for the mass of the scalar hybrid become quite stable and predictable after instanton contributions are included. The mass of the $(\bar{u}ug + \bar{d}dg)/\sqrt{2}$ hybrid is around 1.83 GeV. However, the instanton effects for the sum rules of the $\bar{s}sg$ hybrid are not stable. Although our analysis seems to suggest a heavier mass for the $\bar{s}sg$ scalar hybrid ($m_H \geq 2\,{\rm GeV}$), it still needs further study.

We also considered non-zero width effects for the sum rules. We find that the $(\bar{u}ug + \bar{d}dg)/\sqrt{2}$ hybrid can be compatible with a very small width ($\Gamma = 0.04\,{\rm GeV}$). After considering this effect, the predicted mass increases about 0.05 GeV, and the sum rules become more stable. Larger or smaller width Γ will make the sum rule unstable, but we cannot exclude such a possibility. For the $\bar{s}sg$ scalar hybrid, instanton effects decrease the stability of sum rule a little, but if we consider an appropriate width, the sum rule with instantons can be very close to the sum rule without instantons in the narrow resonance ansatz, which gives a mass at about 2.20-2.30 GeV.

Instantons also can induce the mixing between j_1 and j_2, which leads to a flavor singlet hybrid with mass around 1.9 GeV, while the flavor octet hybrid is not supported by QCD sum rules.

Finally, we studied the mixing effects between scalar hybrid and glueball currents. The mixing between the $(\bar{u}ug + \bar{d}dg)/\sqrt{2}(\bar{s}sg)$ and the glueball causes two states, one in the region 1.4-1.8 GeV(1.4-2.2 GeV), and the other in the range 1.8-2.2 GeV(2.2-2.6 GeV).

Understanding the crowded 0^{++} meson spectrum in the regions 1.3-1.7 GeV and 2.0-2.3 GeV is an important task in particle physics, both in the naive quark model and in non-$\bar{q}q$ meson model. Our result may give possible interpretations of some of these mesons. For example, $f_0(2020)$ is a particle listed in the latest version of Review of Particle Physics that still requires confirmation[47]. Its mass is 1.99 GeV, and width is 0.55 GeV. Notice that our result shows that the flavor singlet scalar hybrid mass is very close to the mass of $f_0(2020)$ with the same quantum numbers. This may lead to a possible explanation that part of the contents of $f_0(2020)$ is a scalar hybrid. Based on our results, even $f_0(1710)$ ($m = 1.72\,{\rm GeV}$, $\Gamma = 0.135\,{\rm GeV}$) may have partial hybrid content.

Acknowledgments

This work is partly supported by K. C. Wong Magna Fund in Ningbo University and NSFC under grant 11175153/A050202.

[1] A. Chodos, R. L. Jaffe, K. Johnson and C. B. Thorn, Phys. Rev. D **10**, 2599 (1974).
[2] R. L. Jaffe and K. Johnson, Phys. Lett. B **60**, 201 (1976).
[3] P. Hasenfratz, R. R. Horgan, J. Kuti and J. M. Richard, Phys. Lett. B **95**, 299 (1980).
[4] T. Barnes, F. E. Close, F. de Viron and J. Weyers, Nucl. Phys. B **224**, 241 (1983).

[5] D. Horn and J. Mandula, Phys. Rev. D **17**, 898 (1978).
[6] I. I. Balitsky, D. Diakonov and A. V. Yung, Phys. Lett. B **112**, 71 (1982).
[7] I. I. Balitsky, D. Diakonov and A. V. Yung, Z. Phys. C **33**, 265 (1986).
[8] S. Narison, Nucl. Phys. A **675**, 54C (2000) [arXiv:hep-ph/9909470].
[9] P. Z. Huang and S. L. Zhu, arXiv:1103.0602 [hep-ph].
[10] H. X. Chen, Z. X. Cai, P. Z. Huang and S. L. Zhu, Phys. Rev. D **83**, 014006 (2011) [arXiv:1010.3974 [hep-ph]].
[11] P. Z. Huang, H. X. Chen and S. L. Zhu, Phys. Rev. D **83**, 014021 (2011) [arXiv:1010.2293 [hep-ph]].
[12] C. F. Qiao, L. Tang, G. Hao and X. Q. Li, J. Phys. G **39**, 015005 (2012) [arXiv:1012.2614 [hep-ph]].
[13] F. Buisseret, V. Mathieu, C. Semay and B. Silvestre-Brac, Eur. Phys. J. A **32**, 123 (2007) [arXiv:hep-ph/0703020].
[14] T. Huang, H. Y. Jin and A. L. Zhang, Eur. Phys. J. C **8**, 465 (1999) [arXiv:hep-ph/9809331].
[15] N. Isgur, R. Kokoski and J. E. Paton, Phys. Rev. Lett. **54**, 869 (1985).
[16] J. Merlin and J. E. Paton, Phys. Rev. D **35**, 1668 (1987).
[17] J. Govaerts, F. de Viron, D. Gusbin and J. Weyers, Phys. Lett. B **128**, 262 (1983).
[18] J. Govaerts, F. de Viron, D. Gusbin and J. Weyers, Nucl. Phys. B **248**, 1 (1984).
[19] J. Govaerts, L. J. Reinders, P. Francken, X. Gonze and J. Weyers, Nucl. Phys. B **284**, 674 (1987).
[20] G. 't Hooft, Phys. Rev. D **14**, 3432 (1976) [Erratum-ibid. D **18**, 2199 (1978)].
[21] T. Schafer and E. V. Shuryak, Rev. Mod. Phys. **70**, 323 (1998) [arXiv:hep-ph/9610451].
[22] M. A. Shifman, A. I. Vainshtein and V. I. Zakharov, Nucl. Phys. B **147**, 385 (1979).
[23] M. A. Shifman, A. I. Vainshtein and V. I. Zakharov, Nucl. Phys. B **147**, 448 (1979).
[24] V. A. Novikov, M. A. Shifman, A. I. Vainshtein and V. I. Zakharov, Fortsch. Phys. **32**, 585 (1984).
[25] P. Faccioli and E. V. Shuryak, Phys. Rev. D **64**, 114020 (2001) [arXiv:hep-ph/0106019].
[26] M. A. Shifman, A. I. Vainshtein and V. I. Zakharov, Nucl. Phys. B **163**, 46 (1980).
[27] H. Forkel, Phys. Rev. D **71**, 054008 (2005) [arXiv:hep-ph/0312049].
[28] A. -l. Zhang and T. G. Steele, Nucl. Phys. A **728**, 165 (2003) [hep-ph/0304208].
[29] M. Shifman, arXiv:hep-th/0009131.
[30] E. V. Shuryak, Nucl. Phys. B **214**, 237 (1983).
[31] A. E. Dorokhov and N. I. Kochelev, Z. Phys. C **46**, 281 (1990).
[32] H. Forkel and M. K. Banerjee, Phys. Rev. Lett. **71**, 484 (1993) [arXiv:hep-ph/9309232].
[33] C. A. Dominguez, Z. Phys. C **26**, 269 (1984).
[34] M. J. Iqbal, X. m. Jin and D. B. Leinweber, Phys. Lett. B **367**, 45 (1996) [arXiv:nucl-th/9504026].
[35] M. J. Iqbal, X. m. Jin and D. B. Leinweber, Phys. Lett. B **386**, 55 (1996) [arXiv:nucl-th/9507026].
[36] V. Elias, A. Fariborz, M. A. Samuel, F. Shi and T. G. Steele, Phys. Lett. B **412**, 131 (1997) [arXiv:hep-ph/9706472].
[37] S. Leupold, W. Peters and U. Mosel, Nucl. Phys. A **628**, 311 (1998) [arXiv:nucl-th/9708016].
[38] B. Kampfer and S. Zschocke, Prog. Part. Nucl. Phys. **53**, 317 (2004) [arXiv:nucl-th/0311042].
[39] G. Erkol and M. Oka, Nucl. Phys. A **801**, 142 (2008) [arXiv:0801.0783 [nucl-th]].
[40] P. Ball and R. Zwicky, Phys. Rev. D **71**, 014029 (2005) [arXiv:hep-ph/0412079].
[41] J. Zhang, H. Y. Jin, Z. F. Zhang, T. G. Steele, D. H. Lu, Phys. Rev. **D79**, 114033 (2009). [arXiv:0903.4029 [hep-ph]].
[42] V. Elias, A. H. Fariborz, F. Shi and T. G. Steele, Nucl. Phys. A **633**, 279 (1998) [hep-ph/9801415].
[43] L. S. Kisslinger and M. B. Johnson, Phys. Lett. B **523**, 127 (2001) [arXiv:hep-ph/0106158].
[44] D. Harnett, T. G. Steele and V. Elias, Nucl. Phys. A **686**, 393 (2001) [arXiv:hep-ph/0007049].
[45] D. Harnett, R. T. Kleiv, K. Moats and T. G. Steele, Nucl. Phys. A **850**, 110 (2011) [arXiv:0804.2195 [hep-ph]].
[46] H. Forkel, Phys. Rev. D **64**, 034015 (2001) [arXiv:hep-ph/0005004].
[47] K. Nakamura *et al.* [Particle Data Group], J. Phys. G **37**, 075021 (2010).